Raman spectra of DRADP-25 dipolar glass: evidence for the mixed ferroelectric - glass phase



1996 J. Phys.: Condens. Matter 8 619

(http://iopscience.iop.org/0953-8984/8/5/011)

J. Phys.: Condens. Matter **8** (1996) 619–629. Printed in the UK

# Raman spectra of DRADP-25 dipolar glass: evidence for the mixed ferroelectric–glass phase

Yu I Yuzyuk†, I Gregora, V Vorlíček and J Petzelt

Institute of Physics, Academy of Sciences of the Czech Republic, Na Slovance 2, 180 40 Prague 8, Czech Republic

Received 20 September 1995

**Abstract.** Raman spectra of a $Rb_{0.75}(ND_4)_{0.25}D_2PO_4$ (DRADP-25) mixed crystal have been investigated in the 8–300 K temperature range for all fundamental polarization geometries. As in the case of DRADP-50, the spectra can be interpreted in terms of vibrational modes of principal structural units. Analysis of the temperature dependence of peak positions and halfwidths has shown two characteristic temperature regions (∼200–220 K and ∼110–120 K) where incipient cluster formation and freezing of individual structural units takes place in this compound on cooling through the dipolar glass transition. In contrast to those for DRADP-50, the Raman spectra of DRADP-25 reveal additionally the onset of incipient ferroelectric clustering and the existence of a low-temperature mixed ferroelectric–glass phase.

## 1. Introduction

$Rb_{1-x}(NH_4)_xH_2PO_4$ (RADP-$x$) and $Rb_{1-x}(ND_4)_xD_2PO_4$ (DRADP-$x$) mixed crystals form dipolar glasses in a large intermediate-concentration range $0.3 \leqslant x \leqslant 0.7$. This ferroelectric–antiferroelectric glassy system has been studied, perhaps more thoroughly than any other one, by various experimental methods (Grimm and Martinez 1986, Grimm *et al* 1986, Courtens *et al* 1984, Korner *et al* 1993, Korner and Kind 1994, Blinc *et al* 1988, Courtens 1986, Martinez *et al* 1987, He 1991, Petzelt *et al* 1993, Yuzyuk *et al* 1995). Its phase diagram is, however, not yet completely understood. In the case of DRADP-$x$ the dielectric dispersion measurements by Kutnjak *et al* (1994) confirmed that the glassy behaviour is most pronounced in the region $0.3 \leqslant x \leqslant 0.65$, whereas possible coexistence of ferroelectric (FE) and glassy regions but the absence of a macroscopic polarization (i.e. long-range FE order) was indicated close to the composition $x = 0.25$. In an NMR study of DRADP-$x$ Korner *et al* (1993) investigated also the compositions on the FE side of the phase diagram ($x = 0.20$, 0.25 and 0.30). They found that while DRADP-20 still undergoes a complete FE phase transition, the transitions for $x = 0.25$ and 0.30 affect only 25% or 10%, respectively, of the volume. The other parts of the volume exhibit short-range glass order with the corresponding dynamics. It seems that the FE clusters or microdomains are still large enough to retain some soft-mode character. At present, however, it is not clear whether this phase segregation is intrinsic or a result of defects or composition striations originating from crystal growth.

IR and Raman spectroscopies provide very useful methods for investigating the freezing of local distortions in the glass state as they provide information about the symmetry

† On leave from the Institute of Physics, Rostov State University, Stachki 194, Rostov-on-Don, 344104, Russia.

0953-8984/96/050619+11$19.50  

displayed in the lattice locally and instantaneously (averaged over a few interatomic distances and a few atomic vibrational periods only). Our recent results on DRADP-50 (Yuzyuk *et al* 1995) illustrate the wealth of data obtained from polarized Raman spectra: in particular, they show that the onset of formation of dynamical clusters should be located at ∼200–220 K and, progressing rapidly on further cooling, the process is completed at a freezing temperature of ∼100 K.

The present contribution reports a similar Raman investigation of a completely deuterated crystal of DRADP-25. Temperature dependences for four scattering geometries corresponding to different symmetry modes in DRADP-25 have been studied from room temperature down to 8 K and their detailed interpretation is given. Particular attention is paid to comparison with the results obtained on DRADP-50 since significant differences were observed in DRADP-25 near the FE transition temperature.

## 2. Experimental details

Raman spectra of DRADP-25 have been measured on a sample in the form of an oriented and carefully polished parallelepiped $4 \times 3 \times 1$ mm$^3$ (with the largest face perpendicular to the $z \equiv c$ crystallographic axis) in the right-angle scattering geometry. The sample was placed in a continuous-flow liquid-He optical cryostat, where it was cooled by convection, permitting us to achieve very good temperature stability over the whole range 8–300 K. The 530 nm line of a $Kr^+$ laser was used for excitation, and the scattered light, collected by a photographic lens, was analysed using a PC-controlled SPEX-14018 double spectrometer equipped with standard photon-counting detection. Identical scanning conditions (laser power, slit width and height) were maintained for all scattering geometries, realized by rotating the polarization of the incident beam, with fixed analyser position. The spectral slit width was ∼2 cm$^{-1}$.

## 3. Results and discussion

### *3.1. Raman spectra at room temperature*

The factor-group analysis of normal vibrations for the KDP-type structure is well known (Courtens and Vogt 1985, Simon 1992). Investigations of the Raman spectra of KDP (Tominaga 1983) showed, however, that the local and instantaneous site symmetry of $PO_4$ tetrahedra above $T_c$ is $C_2$, which is the same symmetry as that below $T_c$, whereas the $S_4$ sites correspond to average positions of the $PO_4$ tetrahedra in the paraelectric phase. Investigations of the Raman spectra of pure DADP at room temperature also show (Kasahara *et al* 1986) that the $D_2PO_4^-$ and $ND_4^+$ ions possess $C_2$ local symmetry. It has been shown (Courtens and Vogt 1985) that the local symmetry of ammonium- and phosphate-ion tetrahedra in RADP-*x* mixed crystals is dynamically broken (dynamic cluster formation) even at room temperature, as is evident from the appearance of lines forbidden by the relevant Raman selection rules. This breaking is, naturally, more pronounced in the glass state.

Isomorphous substitution of $NH_4^+$ for $Rb^+$ (very close values of ionic radii) results in marked perturbations of the local symmetry of both these sublattices in mixed crystals, since each ammonium ion is bound via asymmetric N–H...O bonds with the oxygen atoms in the $PO_4$ groups, which participate in forming the O–H...O bonds (Courtens 1987). Consequently, the ammonium tetrahedra become distorted and shifted away from the $S_4$ site centre, reducing thus the real local symmetry to $C_2$ or $C_1$. This, in turn, leads to distortions of the $PO_4$ groups. All these effects become even more pronounced on deuteration: internal

**Table 1.** Frequencies (in $cm^{-1}$) of observed Raman modes in DRADP-25. $L^P$: $PO_4$ librations; $L^N$: $ND_4$ librations; asterisk: main peaks of $PO_4$ internal vibrations; s: strong; w: weak; vw: very weak; sh: shoulder; ?: uncertain.

| $y(xx)z = A_1 + B_1$ | | $y(zz)x = A_1$ | | $y(zx)z = E$ | | $y(xy)z = B_2$ | | |
|---|---|---|---|---|---|---|---|---|
| 300 K | 8 K | 300 K | 8 K | 300 K | 8 K | 300 K | 8 K | Assignment |
| 55vw | 62vw | | | | | | | |
| 84 | 85 | 80 | | 82 | 84 | 80vw | 85vw | External translations |
| | 93 | | | | | | | |
| | 100vw | | | | 101 | | | |
| 115 | 116vw | | | | 116vw? | 117vw | | |
| | 121 | | | | | | 121vw | $L^P$ |
| | 138 | | | 130 | 134 | | 138vw | |
| 164w | 158vw | | | 169 | 156 | | | |
| 182 | 187 | | | | 191 | 180vw | 188vw | $L^N$ |
| | 236 | 230 | 230 | 226w | | | 234vw | |
| | | | 245vw | | 240 | | | |
| | 303vw | | 301w | | | | 306vw? | |
| | 314vw | | 314w | | | | | |
| **353s*** | 350s | **356s*** | 350s | 355 | 350 | 354 | 349 | $\nu_2^P$ |
| 382 | 382 | | 386 | 386vw | 382w | **382*** | 382 | |
| | 400 | | | | 400w | | 400vw | |
| | 446sh | | | | | | 442sh? | |
| **450s*** | 460s | | 460vw | **466sh*** | 461 | **450*** | 459 | |
| | | | | | 470 | | | |
| 510 | 507 | 509 | 506 | | 508 | 510 | 505w | $\nu_4^P$ |
| | | | | | 518vw | | | |
| | | | | 520 | 530 | | | |
| 545 | 545 | | | **542s*** | 540w | 548vw | 544w | |
| | 558sh | | 554vw | | 553sh | | 553vw | |
| 700 | 700 | 704vw | 700w | 710vw | | 706vw | 708w | $\gamma$(O–D) |
| | | | | | 726w | | | |
| | 870s | | 870s | | 870 | | 870 | |
| **882s*** | 880s | **882s*** | 880s | 882 | 880 | 881 | 880 | $\nu_1^P$ |
| | | | | | 918vw | | | |
| | | | | **930*** | 936 | | | $\nu_3^P$ |
| **961*** | 979 | 958s | 956sh | | | 960 | 960sh | |
| 998 | | 1000sh | 978s | 980 | 978 | 999sh | 980 | $\leftarrow\delta$(O–D) |
| | 1041 | | | 1086vw | | | 1040vw | |
| | 1102 | | 1101vw | | 1102 | | | $\nu_4^N$ |
| | | | | 1177 | | | | |
| 1193 | 1188 | 1190 | 1188 | 1190sh | 1190 | 1193vw | 1188vw | $\nu_2^N$ |
| | 1232vw | | | | | 1220vw | 1230vw | |
| 1340 | 1368 | | | | 1368vw | | 1366vw | $2\gamma$(O–D)? |
| | 1558 | | | | | | | |
| 1750 | 1730 | | | 1760vw | 1750vw | 1735vw | 1750vw | $\nu$(O–D) |
| 1850w | 1842 | | | | | | | |
| 1950 | 1950 | | | | 1960vw | | 1960vw | |
| 2002 | 2020 | | | 2000vw | | 1996vw | | |
| | 2150 | 2150 | 2150sh | 2140vw | 2156w | | | |
| 2154 | 2176 | | 2176 | | | 2188vw | 2176vw | |
| 2246 | 2242 | 2252 | 2242 | | 2243vw | | 2242vw | $\nu_1^N$ |
| | | 2262w | | | | 2250vw | | |
| | 2304 | | 2304w | | 2308w | | | |
| | 2355 | | | | | | | $\nu_3^N$ |
| 2370 | 2384 | | | | 2378vw | | | |
| | | 2396 | 2404w | 2416 | 2424w | 2424vw | | |
| 2442 | 2450 | | 2442w | | 2450sh | | 2450vw | |

modes of the $PO_4$ and $ND_4$ tetrahedra show larger splittings and there is a stronger leakage of the symmetry-forbidden modes.

The overall Raman spectra of DRADP-25 at 300 K and 8 K for four different scattering geometries are shown in figures 1 and 2, respectively; the corresponding frequencies are summarized in table 1.

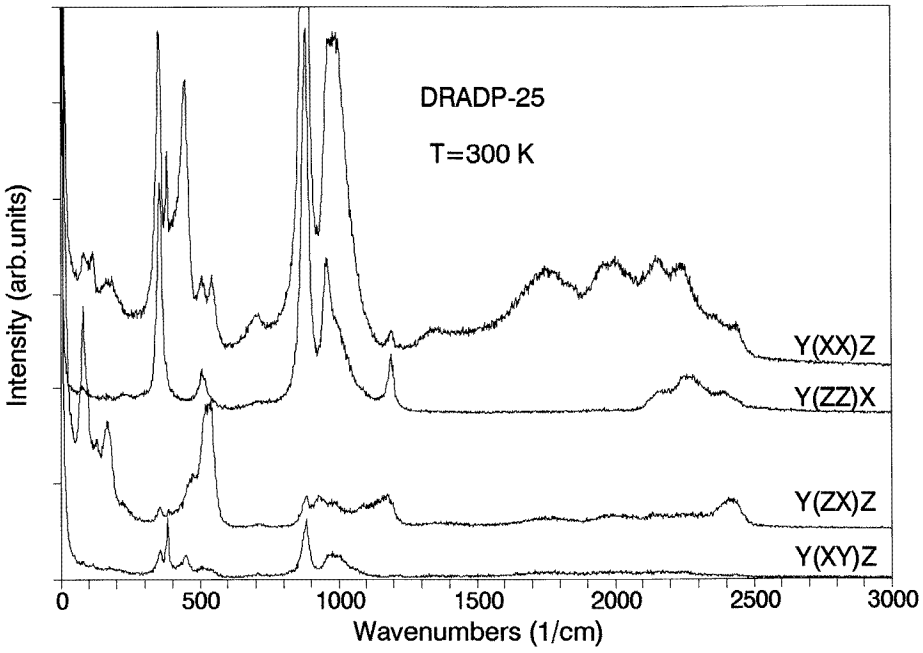


**Figure 1.** Overall Raman spectra of DRADP-25 at room temperature for four polarization geometries.

The room temperature spectra of DRADP-25 closely resemble those of DRADP-50 (Yuzyuk *et al* 1995). The principal difference is, of course, a weaker intensity of all the Raman bands involving the vibration modes of the $ND_4$ group, in quantitative agreement with the difference in composition. The assignment thus closely follows the corresponding discussion given in our preceding paper (Yuzyuk *et al* 1995) on DRADP-50.

### *3.2. Temperature evolution*

The following discussion is organized in a similar manner to that in our preceding paper, i.e. according to individual structural units. The emphasis is on significant differences in the behaviour for both compositions.

*3.2.1. $PO_4$.* On lowering the temperature we observe further increase in the leakage of modes into 'forbidden' polarization geometries and decrease of their width, which indicates a lowering of the anharmonicity of thermal vibrations and a freezing in of all sublattices in general non-symmetric positions. This trend is rather monotonic, but the singularities observed in the temperature behaviour of some parameters make it possible to define in DRADP-50 two temperature regions, namely ∼100–120 K and ∼200–220 K. In DRADP-25,

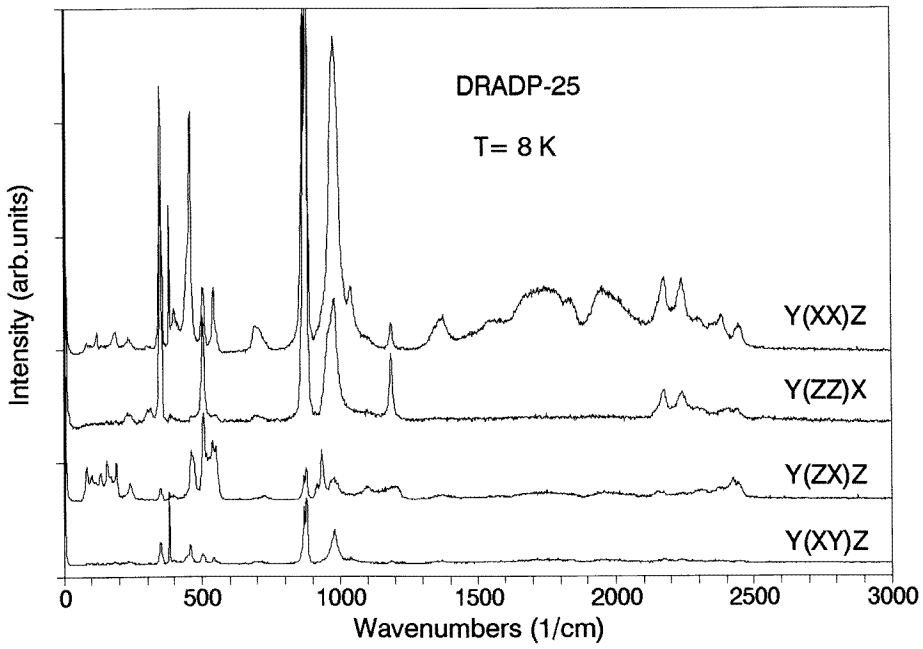


**Figure 2.** Overall Raman spectra of DRADP-25 at 8 K.

however, more abrupt variations than in DRADP-50 are observed near 120–130 K, which is connected with the transition into the ferroelectric phase.

(i) In the DRADP-50 crystal the fully symmetric stretching vibration $\nu_1^P$ splits at low temperatures into two components, at 868 and 882 $cm^{-1}$, as shown in figure 3. This effect has been attributed to the formation of non-equivalent $PO_4^{3-}$ anions having different surroundings at low temperatures because of random distribution of $ND_4^+$ and $Rb^+$ cations in the crystal. We have estimated from the two-oscillator fit of the lineshape of the $\nu_1^P$ peak at which temperature this splitting sets in. Above 120–130 K the lower-frequency component starts to shift upwards and both lines merge into one at about 200–220 K, showing no further frequency variation between 220 and 300 K (figure 4).

In DRADP-25 similar behaviour of the components of $\nu_1^P$ is observed, with the splitting taking place in the same temperature interval. However, the magnitude of the splitting is lower, amounting to 10 $cm^{-1}$ (compared to 14 $cm^{-1}$ in DRADP-50) below 120 K, which can be explained by a lower magnitude of distortion of the $PO_4$ tetrahedra in DRADP-25.

(ii) The bending mode $\nu_2^P$ is known (Courtens and Vogt 1985) to be sensitive to proton (deuteron) ordering because of its torsional character. At the PE $\rightarrow$ FE phase transition in KDP the frequency of this mode drops down by 14 $cm^{-1}$ (Coignac and Poulet 1971) and its halfwidth becomes twice narrower (Laulight 1978), which is due to the attachment of protons to the $PO_4^{3-}$ anion. The temperature dependence of the frequency of the $\nu_2^P$ mode in the *y(zz)x* geometry in DRADP-50 and DRADP-25 is compared in figure 5. Considerable lowering of the $\nu_2^P$ frequency in DRADP-25 between 220 and 120 K is evidently connected with the FE phase transition in the clusters containing $Rb^+$ ions. Analogous behaviour of the $\nu_2^P$ frequency has been observed by Courtens and Vogt (1985) in RADP-35, where the transition near a mixed FE + glass phase takes place, too.

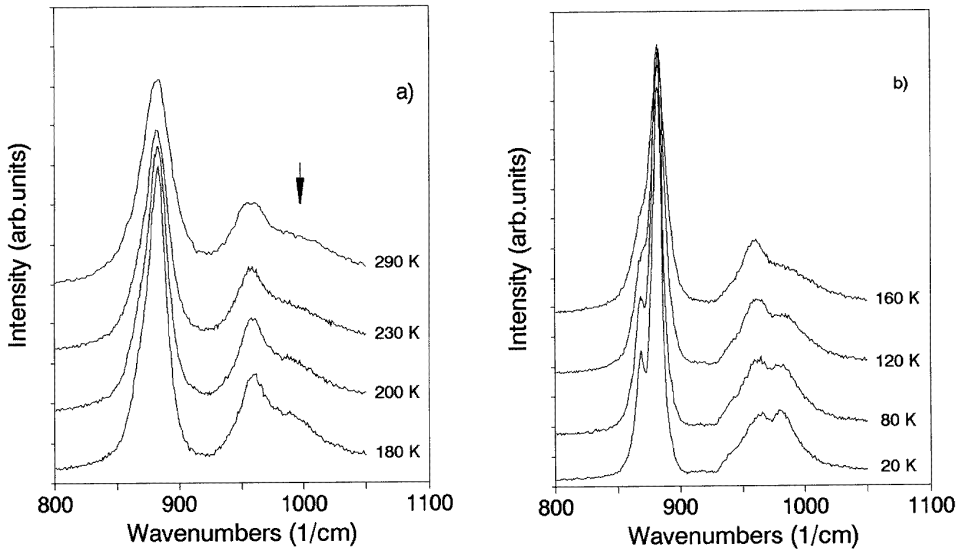


**Figure 3.** The behaviour of the $A_1$ component of the symmetric and antisymmetric stretching vibration bands $\nu_1^P$ and $\nu_3^P$ in DRADP-50 on cooling. The arrow points to a band at ∼990 $cm^{-1}$ (less well resolved at higher temperatures) attributed to the bending vibration of the O–D...O bond.

(iii) An unusual temperature behaviour was observed in DRADP-50 in the region of the $\nu_3^P$ vibrations. At room temperature there are two lines observed in the *y(zz)x* orientation: at 956 $cm^{-1}$ and at ∼988 $cm^{-1}$ (less well resolved peak). On lowering the temperature, the widths of both lines decrease and the high-frequency mode shifts noticeably downwards, until below 120 K a well resolved doublet appears (figure 3). The frequency of the other mode is virtually independent of temperature. If these lines were components of the degenerate $\nu_3^P$ mode, their frequencies would be expected to separate with decreasing temperature. However, as discussed by Yuzyuk *et al* (1995), only the line at 956 $cm^{-1}$ refers to $\nu_3^P$ and the broader line at ∼990 $cm^{-1}$ is a bending mode $\delta$(O–D) of the O–D...O bond. The latter becomes much narrower on decreasing the temperature from 300 to 100 K, and below 100 K its frequency remains practically constant. This behaviour has been interpreted as evidence for the freezing in of the deuterons. The frequencies of the $\nu_3^P$ and $\delta$(O–D) lines in DRADP-50 and DRADP-25 are plotted in figure 6. It is clear from this figure that in DRADP-25 the variation of the $\delta$(O–D) line with temperature in the 120–140 K range is more abrupt, which is also a consequence of the FE phase transition in this mixed crystal.

(iv) As reviewed by Simon (1992), some interaction takes place between the $\nu_4^P$ mode, the Rb–$PO_4$ mode and the ferroelectric mode at FE phase transition in $RbH_2PO_4$. According to this idea of the PE phase transition upon heating from the FE phase, the proton motions lead to partial softening of the $\nu_4^P$ mode, and this softening pushes down the lower-frequency Rb–$PO_4$ external mode, which slightly softens, too, and a partial transfer of the dielectric strength and eigenvectors occurs.

We have performed a detailed investigation of the temperature dependence of this mode in DRADP-50 and DRADP-25 in the $y(zx)z$ orientation, where it is sufficiently well resolved. The temperature evolution of the Raman spectra is shown in figure 7 and the mode

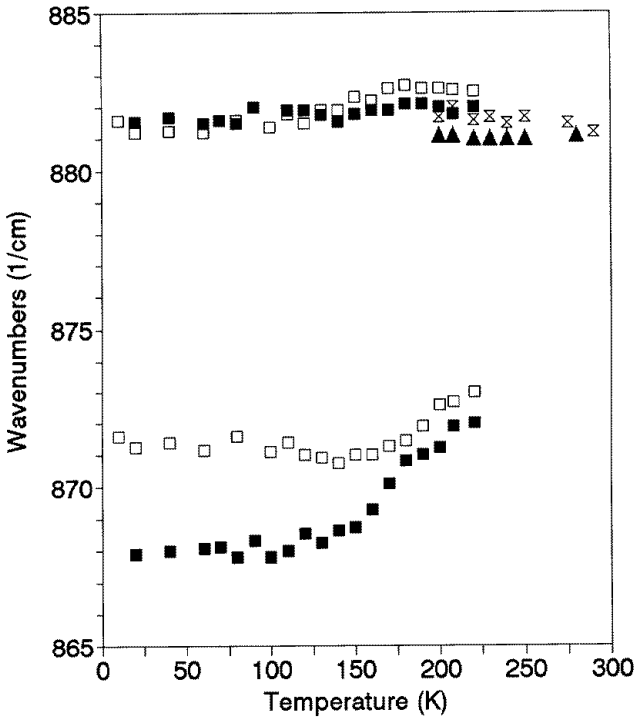


**Figure 4.** The temperature dependence of the frequencies of the two components of the $\nu_1^P$ band in DRADP-50 (full symbols) and DRADP-25 (open symbols), as determined from a two-oscillator fit to the lineshape (squares). The splitting is no longer resolved above ∼200 K and a single-oscillator fit (triangles) becomes equivalent.

frequencies, determined by multi-oscillator (Lorentzian) fits, are plotted versus temperature in figure 8. The fitting procedure deserves a comment: first, the room temperature spectra were decomposed into a minimal set of Lorentzian peaks and the best fits were subsequently used as starting approximations for fitting the spectra taken at decreasing temperatures, occasionally adding new peaks whenever the fit quality (as indicated by the RMS deviation) significantly deteriorated. Then, the procedure was reversed, starting from the low-temperature spectra with a larger set of Lorentzians and removing weak and less well defined peaks as long as the RMS deviation remained satisfactory. Although the fitting procedure is hardly unique, we arrived in this way at a relatively consistent picture, reasonably describing the temperature evolution: the onset of splittings and/or the emergence of new lines should be located in the temperature ranges 100–130 K and 200–240 K, where most of the ambiguities in the number of fitted peaks appear.

The room temperature Raman spectra of both compounds in the 450–600 $cm^{-1}$ range are virtually identical, being composed of two strong lines at 518 and 539 $cm^{-1}$ (DRADP-50) or 517 and 540 $cm^{-1}$ (DRADP-25) and of a weak broad band near 471 $cm^{-1}$ (DRADP-50) or 467 $cm^{-1}$ (DRADP-25). It is clear from figure 8 that in DRADP-50 a splitting of the lines at 518 and 539 $cm^{-1}$ takes place in the temperature range of 220–240 K, where $\nu_1^P$ splits, too (!), whereas the band at 471 $cm^{-1}$ splits near 120–130 K.

In DRADP-25 the lines at 517 and 540 $cm^{-1}$ split in much the same way near 220–240 K into components of very close frequencies, but, in addition, in the 120–130 K range they

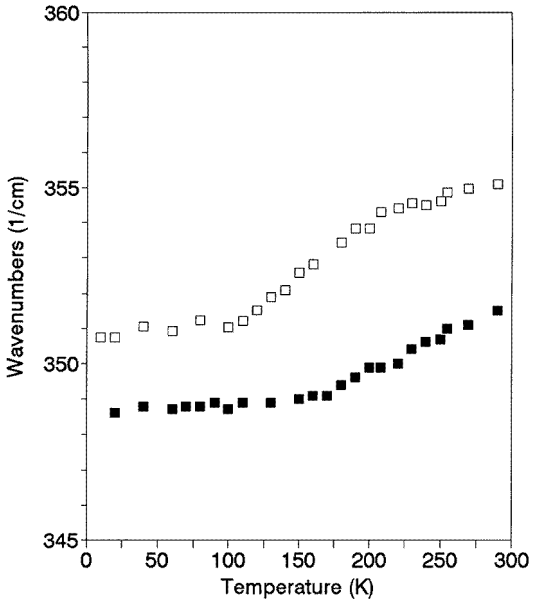


**Figure 5.** The temperature dependence of the frequencies of the $\nu_2^P$ bending vibration in DRADP-50 (full squares) and DRADP-25 (open squares), as determined from a Lorentzian fit to the lineshape.

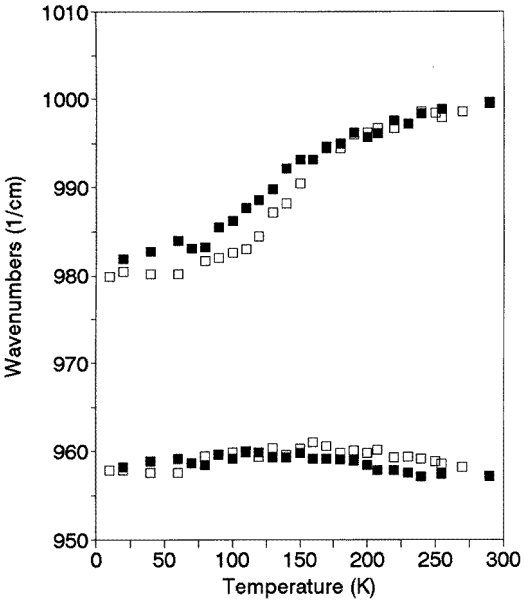


**Figure 6.** The temperature dependence of the frequencies of the $\nu_3^P$ antisymmetric stretching and $\delta$(O–D) bending vibration in DRADP-50 (full squares) and DRADP-25 (open squares), as determined from Lorentzian fits to the lineshape.

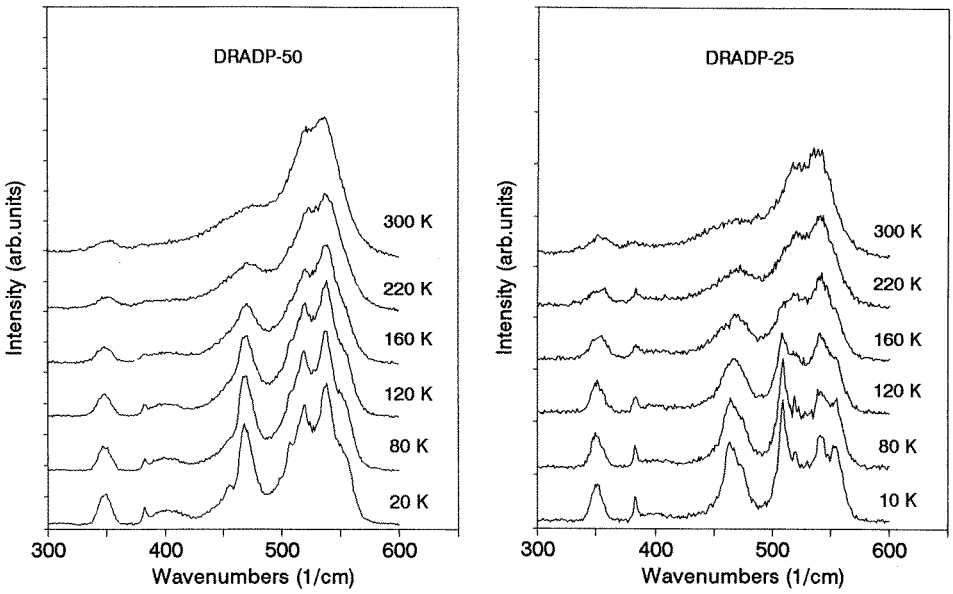


**Figure 7.** The temperature evolution of the Raman spectra in the range of the $\nu_3^P$ bending vibration (E modes) in DRADP-50 and DRADP-25.

split further into a considerably larger number of components than in DRADP-50 and at low temperatures (below 120 K) the spectra in this frequency range look quite different. Below 120 K the Raman spectrum of DRADP-25 is very similar to that of KDP below $T_c$ (Coignac and Poulet 1971), i.e. in the FE phase. The larger number of the $\nu_4^P$ components below 120 K is evidently connected—on one hand—with a lowering of the local symmetry of the $PO_4^{3-}$ anions in the FE clusters or microdomains with a random distribution of local spontaneous dipole moments, and—on the other hand—with the formation of the short-range glass order in the other part of the volume.

Analogous splitting of the $\nu_4^P$ mode was observed earlier in the IR spectra of DRADP-25 (Kamba *et al* 1994) where few extra modes were seen at low temperatures at 501 and 513 $cm^{-1}$ for $\boldsymbol{E}\|\boldsymbol{c}$, but unfortunately this splitting was not studied in detail. It was suggested that these modes are due to partial protonation of the sample surface. We can now conclude that this splitting is rather due to the FE phase transition.

It should be noted that we did not observe any softening of the $\nu_4^P$ components near the FE transition temperature, like that which takes place in $RbH_2PO_4$ (Simon 1992); instead, only a splitting occurs. This is connected with the fact that in deuterated compounds the collective D motion was observed at much lower frequencies (Petzelt *et al* 1993), so there is no appreciable interaction with the $\nu_4^P$ mode. Comparison with the soft relaxation in DRADP-50 and DRADP-25 shows a qualitatively similar behaviour (Kamba *et al* 1994).

*3.2.2. $ND_4$.* Like in DRADP-50, the lines corresponding to the internal $ND_4$ modes (frequency ranges ∼1000–1250 $cm^{-1}$ and ∼2000–2500 $cm^{-1}$) become progressively narrower with decreasing temperature, splitting eventually into a large number of components at low temperatures (below 120 K). This is the consequence of a low ($C_1$) local symmetry of the $ND_4$ ion in the glass state.

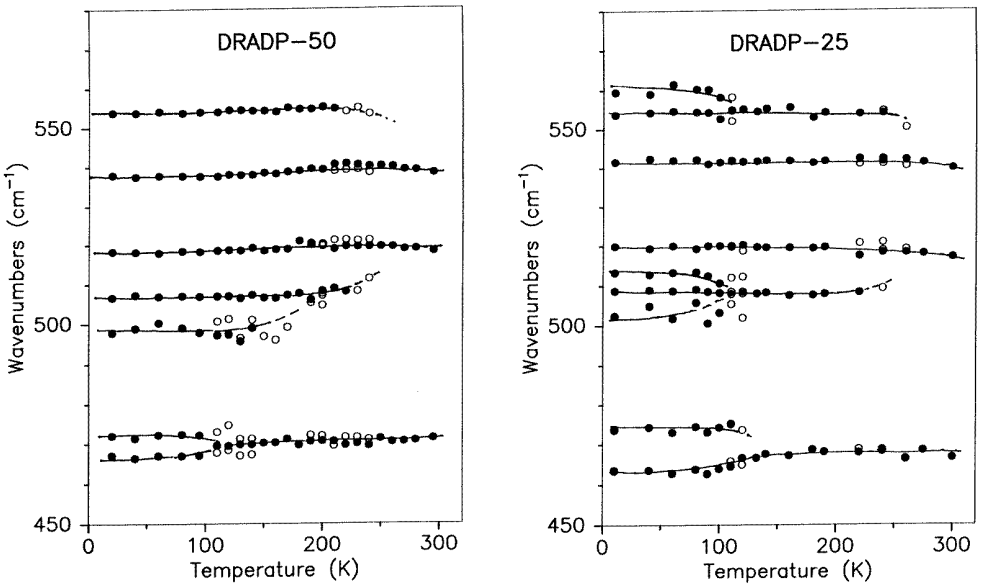


**Figure 8.** The temperature evolution of the frequencies of the components of the spectra of figure 7, as determined by multi-oscillator fits. Open circles denote less reliably determined or additional peaks, when a comparable fit with a smaller number of Lorentzians was possible. The lines through the points are guides to the eye.

*3.2.3. OD.* The frequencies of the O–D stretching modes ($\nu$(O–D), range ∼1500–2000 cm$^{-1}$) do not vary appreciably over the interval of temperatures investigated; consequently, this applies also to bond lengths. Again, like in DRADP-50, the bands remain broad down to the lowest temperature, reflecting the fact that both D and O atoms freeze in disordered positions, so the average potential seen by deuterons shows a broad distribution down to low temperatures.

*3.2.4. External modes.* The spectra of $ND_4^+$ librations (around ∼200 cm$^{-1}$) show similar behaviour to that in DRADP-50. Because of the lower concentration of ammonium, however, their intensity is rather low in DRADP-25. At low temperatures, below 120 K, the range of external frequencies in this crystal shows a wealth of narrower lines (compared to that for DRADP-50), which testifies to the existence of regions with long-range order in the crystal of this composition.

## 4. Conclusion

Like in the case of DRADP-50, in DRADP-25 our results permit us to conclude that incipient cluster formation is located at 200–220 K, where a splitting of the $\nu_1^P$ mode appears in Raman spectra of both compounds. These temperatures correspond to a smeared straight line in the phase diagram of DRADP-*x* connecting the phase transition temperatures of pure DRDP and DADP compounds; this line, however, is not marked (nor established experimentally) on the *T*–*x* diagrams of the system hitherto published (Kutnjak *et al* 1994, Korner *et al* 1993), although some experimental data were known of before: (i) the appearance of incommensurate correlations in neutron scattering, which start to develop below 210 K

(Xhonneux *et al* 1988); and (ii) the onset of broadening of the $ND_4^+$ deuteron NMR lineshapes, observed below 230 K for $x = 0.44$ (Blinc *et al* 1988).

We can suggest that below 220 K in DRADP-*x* solid solutions randomly and independently polarized dynamic clusters start to form, without giving rise to non-ergodicity and long-range order. In dilute ferromagnets this state, the appearance of which is possible below the phase transition temperature of the pure compound, is called Griffiths's phase (Griffiths 1969).

At high concentrations of $Rb^+$ ($x \leqslant 0.2$) a sharp ferroelectric transition occurs in DRADP-*x* at a temperature somewhat below 220 K. From the comparison of the Raman spectra of DRADP-50 and DRADP-25 we can conclude that on further cooling there appears in DRADP-25 a mixed FE + glass phase, in agreement with the results obtained from $^{87}$Rb NMR (Korner *et al* 1993) and dielectric measurements (Kutnjak *et al* 1994).

## Acknowledgments

The authors thank M Ehrensperger and R Kind for providing the DRADP-25 crystal. This work was supported by the Czech Grant Agency (Project No 202/95/1393), and the grant 94-02-03573-a of the Russian Foundation of Fundamental Research.

## References

Blinc R, Dolinsek J, Schmidt V H and Ailion D C 1988 *Europhys. Lett.* **6** 55
Coignac J P and Poulet H 1971 *J. Physique* **32** 679
Courtens E 1986 *Phys. Rev.* B **33** 2975
——1987 *Ferroelectrics* **72** 229
Courtens E, Rosenbaum T F, Nagler S E and Horn P H 1984 *Phys. Rev.* B **29** 515
Courtens E and Vogt H 1985 *J. Chem. Phys.* **82** 317
Griffiths R B 1969 *Phys. Rev. Lett.* **23** 17
Grimm H and Martinez J 1986 *Z. Phys.* B **64** 13
Grimm H, Parlinski K, Schweika W, Courtens E and Arend H 1986 *Phys. Rev.* B **33** 4969
He P 1991 *J. Phys. Soc. Japan* **60** 313
Kamba S, Petzelt J, Železný V, Smutný F, Gorshunov B P, Kozlov G V, Voitsechovskii V V and Volkov A A 1994 *Ferroelectrics* **157** 227
Kasahara M, Tokunaga M and Tatsuzaki I 1986 *J. Phys. Soc. Japan* **55** 367
Korner N and Kind R 1994 *Phys. Rev.* B **49** 5918
Korner N, Pfammater C and Kind R 1993 *Phys. Rev. Lett.* **70** 1293
Kutnjak Z, Pirc R, Lerstik A, Lerstik I, Filipič C and Blinc R 1994 *Phys. Rev.* B **50** 12 421
Laulight I 1978 *J. Phys. Chem. Solids* **39** 901
Martinez J L, Agullo-Rueda F and Schmidt V H 1987 *Ferroelectrics* **76** 23
Petzelt J, Kamba S, Sinitski A V, Pimenov A G, Volkov A A, Kozlov G V and Kind R 1993 *J. Phys.: Condens. Matter* **5** 3573
Simon P 1992 *Ferroelectrics* **135** 169
Tominaga Y 1983 *Ferroelectrics* **52** 91
Xhonneux P, Courtens E and Grimm H 1988 *Phys. Rev.* B **38** 9331
Yuzyuk Yu I, Gregora I, Vorlíček V, Pokorný J and Petzelt J 1995 *J. Phys.: Condens. Matter* **7** 683